AUTOMATED MANUFACTURING OF THERMOPLASTIC COMPOSITE RIVETS

V. Fortier[1,2*], J.E. Brunel[3], L. Laberge Lebel[1,2*]
[1] ACFSLab, Mechanical Engineering, Polytechnique Montreal, Montreal, Canada
[2] Research Center for High Performance Polymer and Composite Systems (CREPEC), Polytechnique Montreal, Montreal, Canada
[3] Aerospace Airframe Stress, Advance Structure Group, Bombardier Product Development Engineering, St-Laurent, Canada
* Corresponding authors (vincent.fortier@polymtl.ca, LLL@polymtl.ca)

ABSTRACT

Strong and light composite materials are used to increase the performance of aircrafts. Composite structures are currently assembled with heavy titanium fasteners since aluminum corrodes in the presence of carbon fibers. An innovative assembly technology using carbon/PEEK thermoplastic composite rivets is proposed. These rivets are heated above their melting temperature and molded in the drilled hole through the components to be assembled. During compression molding, the resin flows and effectively seals the joint. The similarity of the materials provides a solution to the corrosion and electromagnetic shielding. However, the riveting technique must be automated to ensure a constant quality in an industrial perspective. An automated riveting machine has been designed and built using a linear electric actuator. The force and displacement of the linear actuator can be controlled to ensure good joint quality and geometry. This machine enables the high speed forming of the thermoplastic composite rivet in a single lap-shear testing assembly. Carbon/PEEK and Carbon/Nylon blanks were riveted. Assembled rivet microstructure was assessed by microscopy. From mechanical test results of the carbon/PEEK rivets, it was observed that the joint's shear strength is comparable to typical aerospace grade aluminum solid rivet. Furthermore, composite rivets are 65 % lighter than titanium fasteners. With these advantages, this technology could be used in the next generation of lighter, cleaner and safer aircraft.

1 INTRODUCTION

Composite materials properties are attractive for aerospace application due to their high specific stiffness and strength. However, new challenges arise when assembling composite components: corrosion, installation damage, electromagnetic shielding and humidity penetration [1], [2]. At the moment, no perfect solution exists to combine structural advantages of composite materials, such as carbon/epoxy, and the simplicity of manufacturing and riveting aluminum structures. Aluminum and carbon fibers are a strong galvanic couple that can promote corrosion. Therefore, heavy and complex titanium bolt assemblies are used. Titanium bolted joint is the most common composite joining method in the aerospace industry [2]. In order to minimize cost and weight, carbon/Polyether Ether Ketone (PEEK) bolts were developed [1]. Hutchins *et al.* have demonstrated their potential into rotor-induced vibration area. The composite bolts were flight tested in helicopters' secondary structures.

Another approach consists of compression-molding a thermoplastic composite rivet into the composite components to be joined [3]. A carbon/PEEK rivet is melted and molded in the drilled hole through the joint. In that perspective, the manufacturing parameters are very similar to compression molding. Generally, the compression molding process is made in four steps: Heating, Consolidation, Solidification and De-Molding. In these process, the critical parameters are the process temperature (T_P), forming pressure and consolidation time. These have a significant effect on consolidation quality and mechanical properties [4]. For aerospace applications, voids content below 2 % is mandatory. To melt and form PEEK thermoplastic composites, a T_P between 370-400 °C in the matrix must be reached [5, 6]. However, cross-linking of PEEK can occur above 450 °C with an

exposure time longer than 15 minutes [5]. Ye *et al.* have studied the compression molding of unidirectional laminates made from carbon/PEEK commingled fibers. They suggest that the compression molding pressure must be over 3 MPa to minimize the consolidation time below 10 minutes with a T_P of 380 °C [4].

If a high forming temperature is essential for forming carbon/PEEK, it is also potentially detrimental to the composite material near the thermoformed rivet. At high temperature and for a given exposition time, a polymer matrix can be modified and even degraded. For thermoset epoxy matrices, it is generally accepted that the degradation occurs at temperature higher than the glass transition temperature (T_g) [6]. Epoxy degradation is an issue for the joint's strength. The T_g of DGEBA epoxy used in the aerospace composites is approximately 180 °C [7]. Moreover, the process must minimize the heat-affected zone in the composite plates. To achieve PEEK melted state, heat can be applied from an external heat source or generated within the composite itself. Joule heating with carbon fibers as the heating element can be used as an internal heat source. This heating technique has been demonstrated for thermoplastic composite welding [8]. The carbon fibers acts as a resistor and generates heat when submitted to a DC current. Any type of carbon fiber-reinforced thermoplastic composites can be used for this application. However, the amount of heat is dependent of the composite's electrical resistance.

Aerospace structure joint design relies on experimentally characterized allowables. Several tests are made to determine the statistically safe limit of a fastened joint, such as NASM1312 for fastener test methods [9]. Tests are performed for several types of fastener, diverse geometries or different materials. The allowables are reported in terms of maximum load per fastener that can be sustain for each configuration. Typical fastener allowables can be found in the Military Handbook, chapter 8 [10].

This study proposes an innovative solution for composite joints technology. An automated thermoplastic composite riveting process was developed using joule heating. Thermal modelling was used to verify the temperature distribution in the rivet and joined members during heating to forming temperature. Rivet morphology was characterized and riveted joints lap shear strength was measured. The studied final geometry has a countersunk head (CSK) on one side and a cylindrical head on the other.

2 EXPERIMENTAL

2.1 Rivet Architecture and Materials

The riveting process developed is similar to compression molding and uses short pre-consolidated rods, referred to as the rivet blanks. The blanks have a diameter of 4.76 mm and a length of 36.5 mm. They are manufactured using unidirectional parallel hybrid yarns of carbon fibers (IM7 or AS4, Hexcel) and PEEK (150, Victrex) or from Pyrofil/polyamide (PA) commingled yarns (Dualon, Karijene Inc). Table 1 presents the physical properties of the blanks. The blanks were made by pultrusion using the same equipment and procedure described in Lapointe *et al*. [11]. Table 1 shows also pultrusion set points depending on the type of matrix.

	PA	**PEEK**
Matrix's Glass-Transition Temperature (°C)	N/D	143
Matrix's Melting Temperature (°C)	215	343
Process Temperature (°C)	240-240	370-400 [5]
Contactless Preheater (°C)	200	300
Contact Preheater (°C)	200	380
Impregnation system (°C)	250	380
Cooling Die (°C)	185	150
Pulling Speed (mm/s)	50	50

Table 1. Blanks' physical properties and pultrusion set points described in Lapointe *et al*. [11]

2.2 Riveting machine set-up

The riveting machine principal elements are schematized at Figure 1a). The driver electrode motion is actioned using a linear actuator (KK6010P200A1F1CS00, Hiwin) with a servomotor (FRLS10205A4A, Hiwin). The motion of the driver electrode is applying the riveting force. A bucking tool and a bucking tool socket act as a mold with a variable shape; the bucking tool can slide away from the joint while being guided by the bucking tool socket. Final joint will be made with carbon/epoxy plates. For first experiments, stainless steel joint were used. Stainless steel has similar thermal properties to carbon/epoxy plates. Therefore, it is expected that similar thermal dissipation in the joint would occur in a composite joint. An external heating in the base helps to reach T_P faster by concentrating the heat in the CSK area. Insulated base avoids electrical current leakage in the epoxy plates. This limits heat generation by Joule effect from the carbon fibers in the carbon/epoxy plates. Table 2 shows the materials used for each main part. The bucking tool is made of two layers of different material to insure an electrical insulation between the driver and all the riveting set-up. For that purpose, alumina ceramic was used for its good electrical insulation and wear properties. The external layer acts as a heat sink.

The driver and heated bed/electrode are the two electrodes that input resistive heating. It is possible to generate heat with only a constant 10 A DC source (AB-3010, Abra) combined with the carbon fibers' resistivity. This electrical power in mostly converted in heat. However, the different tooling configurations provide different cooling capacities. This allow to concentrate the heat generated in the blank's section to be formed. To heat the CSK side, the air layer between the blank and the CSK cone, decreases the cooling capacities on CSK's side (see white triangles seen in Figure 1b). Therfore, heat can be generated more efficiently and T_P can be reached locally before heating the composites plates. The same phenomenon happens when the bucking tool goes up before forming the head, as seen Figure 1d). The riveting set-up measures and records five process parameters with LabVIEW (National Instrument) and a DAQ (U6, Labjack), i.e., the blank's temperature, the joint's temperature, the linear actuator's position, the riveting force and the electrical power supply by the source. Temperatures are measured with two K-type thermocouples, one in the heated bed electrode (defined as the blank temperature) and one in the joint. These thermocouples are connected to a PID thermal controller (CN7523, Omega). One PID controls the heated base temperature and the other only acquires the joint's temperature. The servomotor controls linear actuator's position and force. The generated power is calculated by measuring the voltage of the DC source with a DAQ.

2.3 Riveting sequence

Figure 1 shows the five steps of the riveting sequence. Figure 2 illustrates typical parameters variation during a complete riveting cycle. In step a), a composite blank rod is inserted in the composite plates. The bucking tool and the bucking tool socket are brought in firm contact with the joint. In step b), a DC current flows in the blank to generate heat by Joule effect. Simultaneously, the heated base is heated to a temperature set point of 380 °C (300°C for PA matrix). During this step, a resistive contact force, approximately 25 N, is applied to ensure a good electrical contact between the electrodes and blank. Excessive force during heating could result into a premature or uncontrolled deformation of the blank. In step c), when T_P is reached, a riveting force of 200 N (11 MPa) is applied on the blank to form the CSK. This step results in a diminution of the blank's length. In step d), the resistive contact force is reapplied and the base stops heating. The bucking tool is raised at high speed actioned by a set of springs (not shown on drawing). This creates a mold cavity for the head of the rivet. The heat is concentrated in the head region due the modified thermal conductivities around the blank. Solid components and plate surfaces in contact with the blank have a higher heat extraction rate than the air within the cavity created by the bucking tool extraction. In step e), a final riveting force is applied when T_P is reached in the upper part of the blank and resistive heating is stopped. The molding force is maintained until the end of the solidification step. When the temperature reaches the T_g of PEEK or below, the joint can be de-molded.

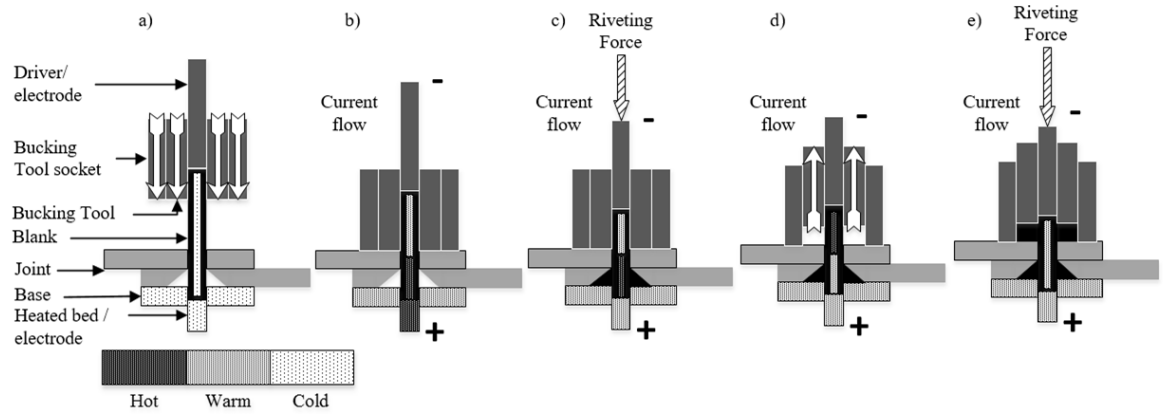

Figure 1. Riveting sequence a) Blank insertion b) Resistive heating c) CSK formation d) Bucking tool opening e) Head formation

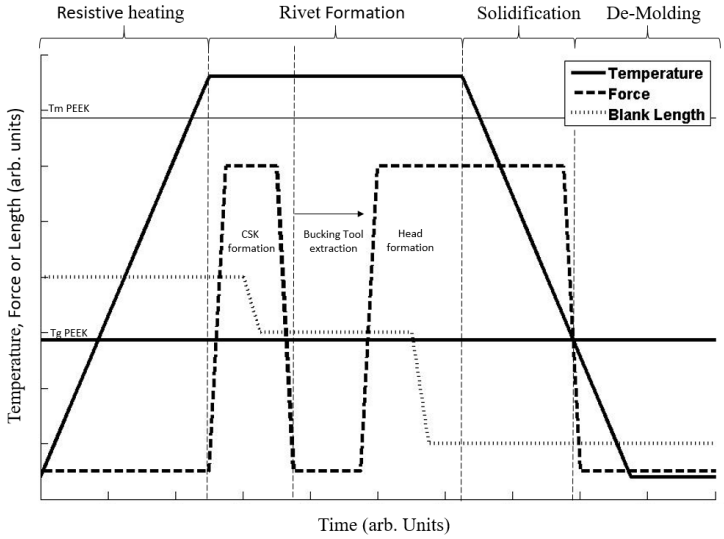

Figure 2. Riveting temperature, force and blank length variation during a typical cycle. Arbitrary units.

Riveting machine parts	Materials	Electrical Conductivity	Thermal Conductivity	Wear
Driver/electrode	W1 tool steel	High	High	Good
Bucking tool socket	Glass-Mica Ceramic	Insulation	Low	N/A
Bucking tool (external layer)	AISI4140	High	High	Good
Bucking tool (internal layer)	Alumina Ceramic	High	High	Good
Base	Glass-Mica Ceramic	Insulation	Low	NA
Heated bed/electrode	360 Brass	Very High	Very High	N/A

Table 2. Materials used for each machine part

2.4 Mechanical and Morphological Characterization

2.4.1 Mechanical test

Single lap shear test were conducted according to the NASM1312-4 standard. The optional configuration with one fastener was used with 4.76 mm thick stainless steel plates. Three samples were tested using a MTS Insight traction machine quipped with a 50 kN load cell. Constant displacement rate of 4 mm/min was applied.

2.4.2 Morphology analysis

Transverse cross-sections of blanks and rivets were polished and observed under a microscope (Eclipse ME600, Nikon). Cross-section are a result of photo merging of 25X magnification. Image processing of 200X and 25X magnifications were used to measure the fiber (V_f) and void (V_v) volume fractions in the composite (ImageJ, open source) [12]. For each area studied, 10 random pictures of the cross-section were taken and analyzed by adjusting the grey level threshold to isolate voids (blacks), matrix (greys) and fiber (whites) pixels. Student's probability law was used to exclude aberrant values with a degree of confidence of 95 %.

3 Results and Discussions

3.1 Process Performance

Figure 3 shows experimental data from a AS4/PEEK riveting process. Heating duration was 5 minutes and was the longest part of the cycle. Higher current source or higher power in the heated bed can decrease the heating time. Internal heating by Joule's effect is suspected to minimize the heat impact on the epoxy. As seen in Figure 3, T_P was reached before the temperature of the plates increase above the epoxy's T_g. When T_P was stabilized, the riveting force was applied and a 3 mm deformation of the blank occurred. It corresponded to the CSK formation. Then, the bucking tool was rapidly lifted and a second resistive contact force was applied to melt the head section. The riveting force was re-applied and a bigger displacement occurred for the head formation. Fast forming speeds are attributed to complete melting of the blank. During the heating step, it is important to reach the T_P, before applying the riveting force. It could result into a badly shaped rivet. When the formation occurs, the melted area will deform until it touches the epoxy plates which are colder than the T_m of PEEK. The matrix will freeze and no more deformation will occur. It is therefore mandatory to ensure complete melting in the deformation area and apply a rapid the riveting motion. A fully automated process insures high forming speed and repeatability to avoid these problems. Future improvement of the process will be tackle the detection of the moment when the matrix is melted. This is critical to improve the forming quality and minimize the rivet formation time.

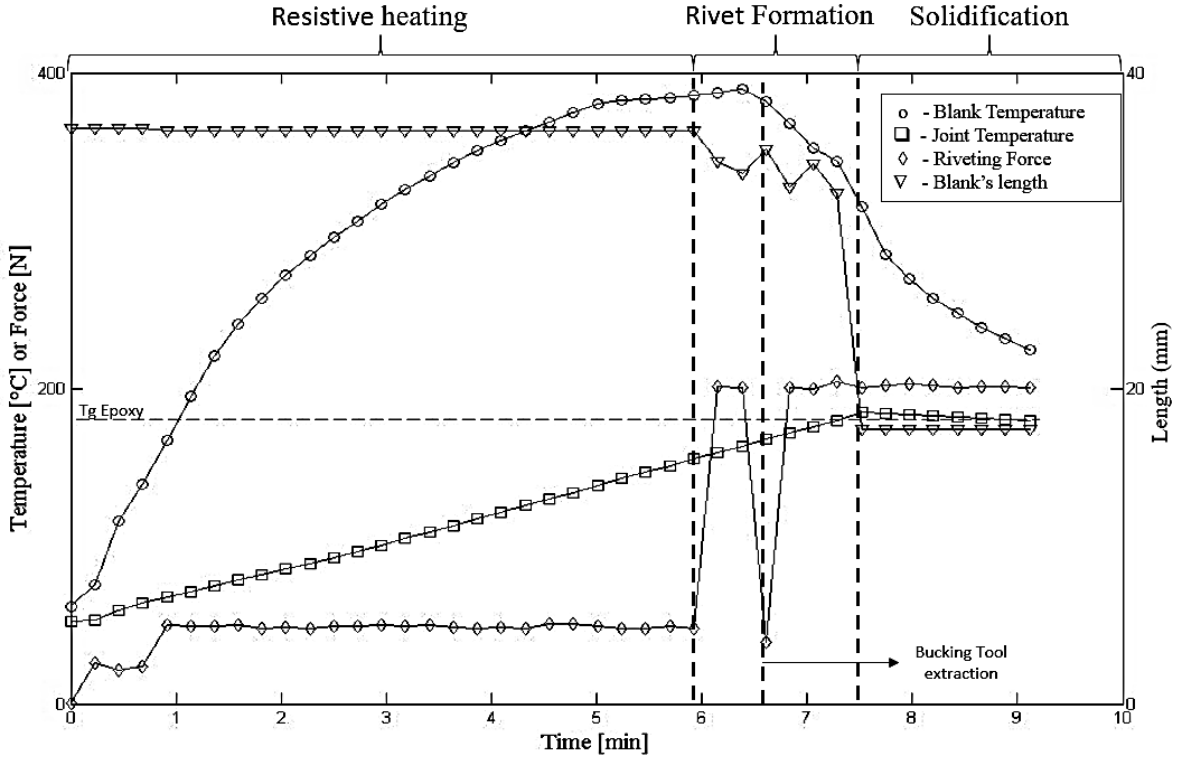

Figure 3. Experimental parameters' variation during the process

3.2 Thermal Simulation

A transient thermal finite element analysis using Ansys Workbench was conducted. The goal was to evaluate the temperature distribution in the riveted joint, during the process. Table 3 and Figure 4a) show the materials used in the assembly and their main physical properties. All materials are considered isotropic except for the blank. The blank, made of unidirectional composite along its length, have higher axial thermal conductivity than transverse. Two 3D models have been done, one for the CSK formation and one for the head formation. Models include an external generated heat of 400 W by the heated base, natural convection of 5 W/m^2°C on all external faces and an ambient temperature of 20 °C. The model also included an internal heat generation between 50 to 80 W. The heating power is modulated with temperature increase. At ambient temperature, an electrical power consumption by the blank of 80 W was measured. At T_P, the power consumption decreased to around 50 W. Using these measured powers, it was assumed that all the electrical power generated by the source was converted into heat generation. Finally, heat generation variations with temperature is assumed linear between ambient and T_P.

The simulation results, shown in Figure 4b) and c), illustrates the temperature distribution before CSK formation and head formation. The temperature zones are delimited by the T_P of PEEK and the T_g of epoxy. To be able to mold the CSK, T_P must be reached in all the section of the CSK area, as shown in Figure 3c). The same approach is considered for the head, as shown in Figure 4d). Temperature distributions can be validated by the temperature acquisition in the Figure 4. More importantly, the temperature distribution can validate the small heat-affected zone on the composite plates. As seen in Figure 4c), the zone above T_g in the epoxy plates have a diameter of 10 mm only. This is similar to the maximum temperature of 185 °C logged during a test (see Figure 4). It is not possible to conclude that the joint will not be mechanically affected by the heat, but the process can minimize this impact.

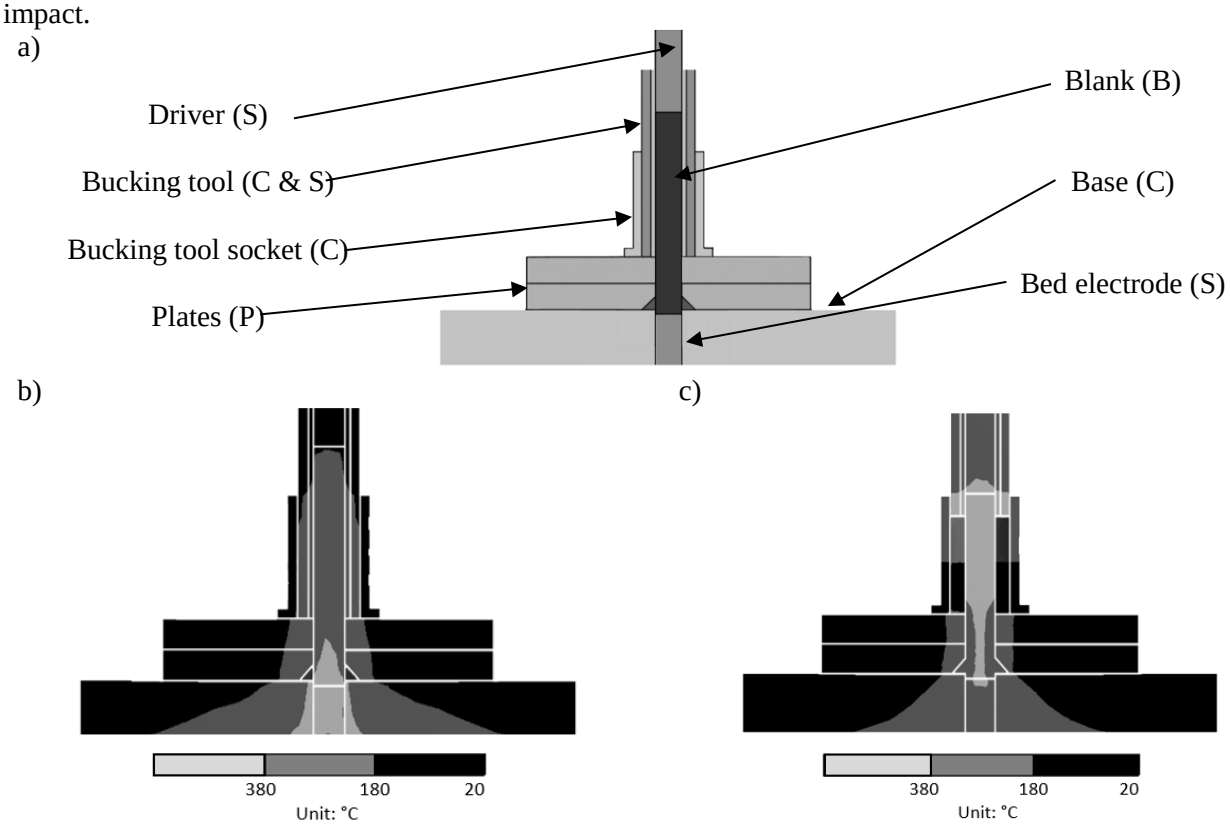

Figure 4. a) Materials' definition b) Temperature distribution before CSK formation d) Temperature distribution before head formation

	Thermal conductivity (W/m°C)	Density (g/cm^3)	Heat capacity (J/kg°C)
Steel (S)	44	7.8	465
Ceramic (C)	1	2.5	1000
Plates (P)	15	7.9	510
Blank axial (B)	30	1.6	950
Blank transverse (B)	1	1.6	950

Table 3. Thermal properties used in the thermal analysis

3.3 Geometry and Morphology Analysis

Figure 5 shows the internal morphology of a blank and a rivet. Table 4 lists the measured fiber and void volume fractions of each cross-section. The Pyrofil/PA pultruded blank and rivet, shown in Figure 5a) and c), have been used to show the result of a well impregnated and formed rivet. Figure 5a) shows low void contents and a parallel placement of the carbon fibers. Figure 5c) illustrates the fiber placement in the rivet's deformed region. Also, it shows a buckled fiber arrangement in the head and CSK due to fiber deformation under the riveting pressure. Poor impregnation quality of the PEEK blank results in a high void content in the rivet, as shown in Figure 5b) and d). Also, PEEK rivet is not formed as well as the PA rivet. This could be attributed to the higher viscosity of the PEEK at the selected T_P. A PEEK T_P of approximately 380 °C was selected. This is only 37 °C over the melting temperature (T_m) of the PEEK. For PA, the T_P was 300 °C, which is 85 °C over the T_m of PA. The lower margin between T_m and T_P is probably responsible for a higher polymer viscosity. The forming quality of the PEEK rivet could improve with higher forming temperature, higher forming pressure or better process control.

The rivet's middle part, the shank, has not changed during the riveting process. The process does not really affect this zone. The heat is only and sequentially concentrated in the CSK and the head. Therefore, the body does not reach a temperature high enough to be deformed. Also, this section is one of the most important for the shear properties of the joint. Therefore, a blank with good consolidation quality (low void content) will lead to a rivet with higher mechanical properties. Furthermore, the fiber placement in the extremities of the rivet could have an impact on the out of plane properties of the joint. In order to obtain repeatable mechanical properties, random fiber placement should be avoided. A bi-axial braided fiber yarn arrangement could be used. Bi-axial braids' diameter tend to increase under compression without losing the intertwined yarn arrangement.

Table 4 shows the constituent analysis made on the blanks and formed rivets. It is seen that the fiber volume fraction greatly differs from the nominal values reported in Table 1. For the Pyrofil/PA blanks, this difference is explained by loss of carbon fiber during pultrusion experiments [11]. For the AS4/PEEK blanks, this difference is attributed to fiber pull-out during the polishing procedure. The carbon fibers were parallel to the polishing surface. Therefore, the poorly impregnated zones cannot secure the fibers during polishing leading to an apparent macro-void creation. Higher standard errors were observed due the random macro-voids dispersion in the microscopies. Since the standard errors are rather high, no conclusion can be drawn at this point on the process' effects on the fiber volume content variations. It is also seen that the void contents in the Pyrofil/PA blanks and rivets do not change significantly before and after the riveting process. However, the PEEK rivet shows that CSK and head formation help to decrease the number of voids in both areas. The riveting force creates a high pressure (11 MPa) which compresses the voids present after production of the blanks by pultrusion. A significant decrease of void content is observed: 47 to 12 %, seen in Table 4. Overall, with enough impregnation of the AS4/PEEK blank, it is suspected that the same consolidation quality will be achieved than for the Pyrofil/PA rivet.

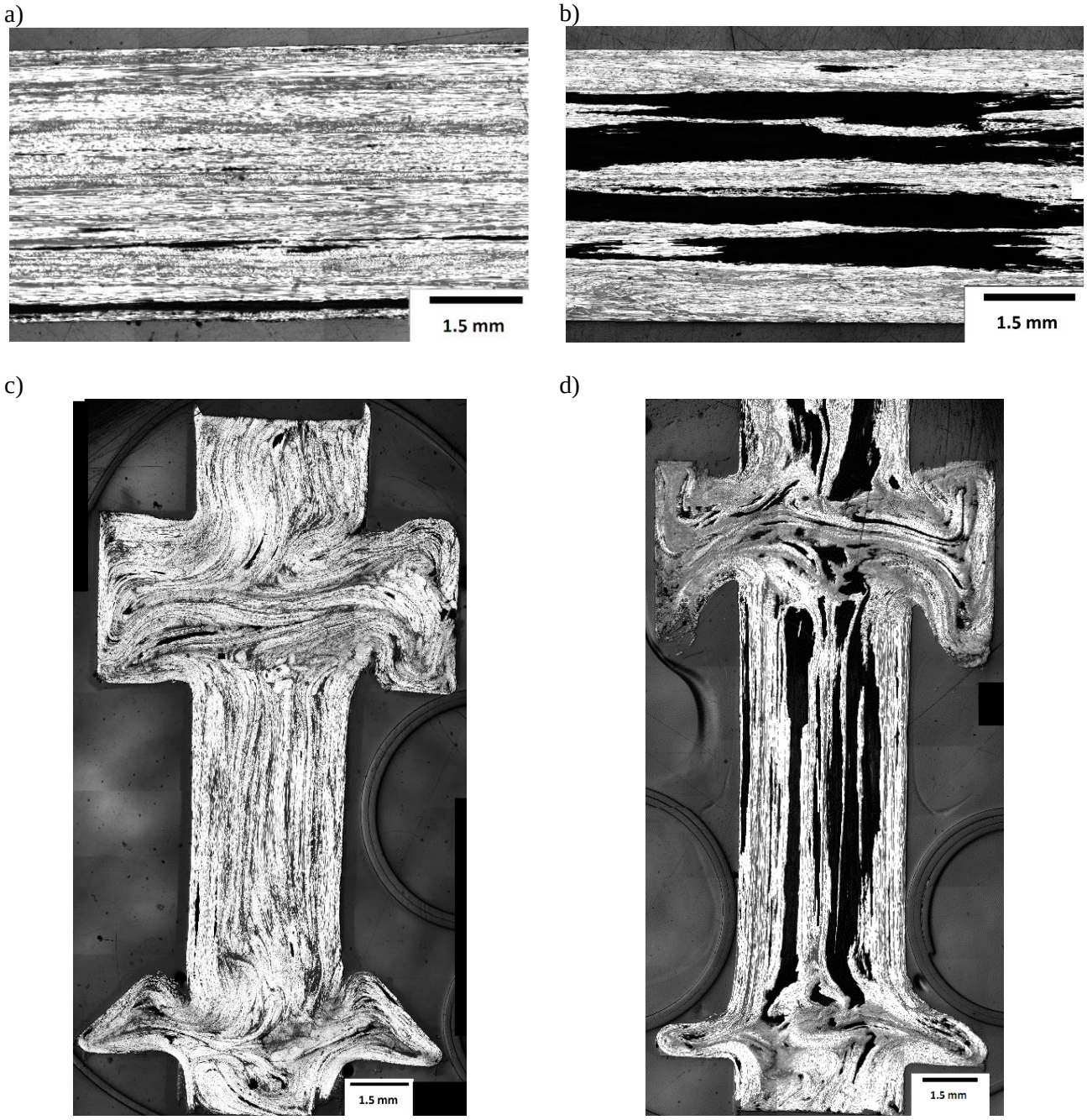

Figure 5. a) Longitudinal cross-section of Pyrofil/PA blank b) Longitudinal cross-section of AS4/PEEK blank c) Longitudinal cross-section of Pyrofil /PA rivet d) Longitudinal cross-section of AS4/PEEK rivet

	Pyrofil/PA (Avg. ± Std. dev.)				**AS4/PEEK (Avg. ± Std. dev.)**			
	Blank	**Head**	**Shank**	**CSK**	**Blank**	**Head**	**Shank**	**CSK**
V_f (%)	44±4	51±10	53±6	53±12	37±4	49±8	34±18	54±13
V_v (%)	1.2±0.6	0.4±0.2	0.4±0.2	0.7±0.8	47±8	12±4	39±24	12±12

Table 4. Constituents' volume fraction

3.4 Mechanical Proprieties

Figure 6 shows an average of three lap shear joint test results. Error bars are the standard deviation calculation at equally spaced experimental points of the three tests. A non-linearity can be seen in the curve. The first part of the curve is attributed to test rig alignment and some rivet rotation. Rivet rotation can amplify out-of-plane loads in the rivet. In the middle of the curve, the load tends to deform the rivet linearly. In the final part, at high loads, the plates bend due to the force misalignment of a single fastener shear test. Also, damage accumulation in the composite rivets change the joint's mechanical behavior. Finally, a ductile rupture occurred after the peak load. It is seen that the standard deviation increase dramatically after peak load and during damage progression. This indicates that the mechanical behavior after the peak load is non-constant and random.

An average peak load of 4484±45 N was measured before the complete rupture of the IM7/PEEK rivets. The experimental fiber and void content are not known. The fiber and void volume fraction should be similar to AS4/PEEK. Each test has the same mechanical behavior and a peak load within the same interval. This repeatability in the peak load proves that the fiber buckling in the head and in the CSK do not affect the shear strength of the riveted joint. Also, Table 5 compares the composite rivet to typical aluminum solid rivet allowables extracted from the Military Handbook, chapter 8 [10]. The riveted joint developed in this study has comparable shear strength to aluminum riveted joint. With a better impregnation, the shear properties of the joint should increase by a significant margin. In future tests, the preferred test in the NASM1312-4 standard will be used with two rivets on each joint. The goal is to minimize the out of plane forces to have comparable data with the solid aluminum rivet properties. Hence, the shear strength will be more representative of the real joint.

Materials	**Single Shear Strength (N)**
5056-H32	3567
2117-T4	3825
IM7/PEEK 50%	**4484**
2017-T4	4826
2024-T4	5227
7050-T73	5471

Table 5. Single Shear Strength for aluminum solid rivet in comparison with the IM7/PEEK rivet

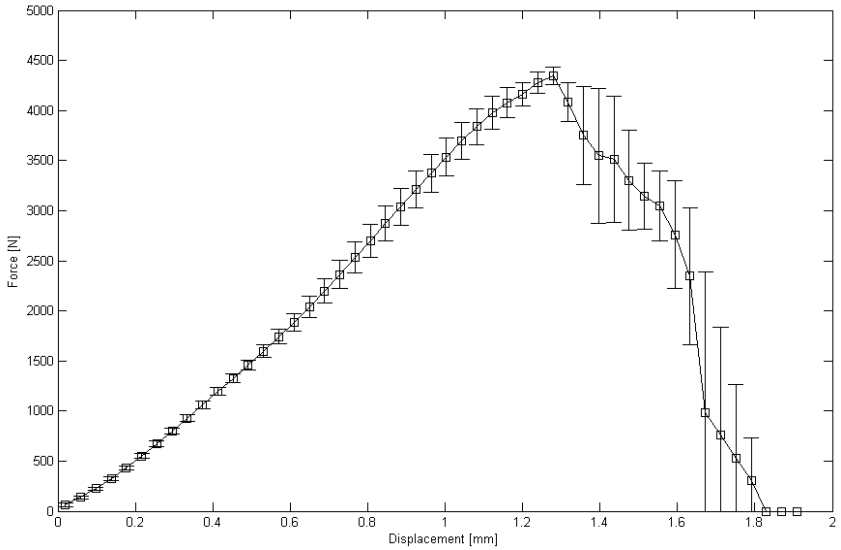

Figure 6. Mechanical behavior of IM7/PEEK during a Lap Joint Shear test of composite rivet according to NASM1312-4 standard for a rivet size of 3/16 inches. Error bars are calculated on an average of three tests.

4 CONCLUSION

An innovative joining process for composite parts was developed using carbon/PEEK rivet. Process parameters have been defined to prove the feasibility of this riveting technology. Voids content can be reduced by the riveting force. Emphasis on the heating design shows the importance of differential cooling capacities to minimize heat-affected zones in the carbon/epoxy plates. Mechanical shear properties of IM7/PEEK rivet are comparable to aerospace grade aluminum solid rivet. Shear properties of the joint are suspected to increase with well impregnated carbon/PEEK blanks. Also, some improvements to the process parameters could minimize the heat-affected zone around the rivet. A biaxial braid could also be used to minimize fiber buckling in the head and CSK. Braiding angle could also increase the shear strength properties of the rivet. These rivets could find application in secondary structure joining of composite aircraft structures.

ACKNOWLEDGEMENT

The authors would like to thank Bombardier Aerospace, Pultrusion Technique, NSERC (CRDPJ488387-15) and Prima Quebec for financing this research project. The authors would also like to acknowledge the contribution of Félix Lapointe for the carbon/PEEK and carbon/PA pultruded blanks.

REFERENCES

[1] J. G. Hutchins, "Update of Composite Fastener Technology at BHTI," 1991.

[2] S. D. Thoppul, J. Finegan, and R. F. Gibson, "Mechanics of mechanically fastened joints in polymer–matrix composite structures – A review," *Composites Science and Technology*, vol. 69, no. 3–4, pp. 301–329, Mar. 2009.

[3] P. Trudeau, L. Laberge Lebel, A. Landry, and D. Hoste, "Composite rivet/fastener blank in aircraft to secure composite unit together, has elongated body where braided reinforcement fibers that are embedded inside body and supported in matrix material are configured to extend length of body.," WO 2015/132766 A1, 11-Sep-2015.

[4] L. Ye, K. Friedrich, J. Kästel, and Y.-W. Mai, "Consolidation of unidirectional CF/PEEK composites from commingled yarn prepreg," *Composites Science and Technology*, vol. 54, no. 4, pp. 349–358, Jan. 1995.

[5] C. M. Stokes-Griffin and P. Compston, "The effect of processing temperature and placement rate on the short beam strength of carbon fibre–PEEK manufactured using a laser tape placement process," *Composites Part A: Applied Science and Manufacturing*, vol. 78, pp. 274–283, Nov. 2015.

[6] A. Chatterjee, "Thermal degradation analysis of thermoset resins," *J. Appl. Polym. Sci.*, vol. 114, no. 3, pp. 1417–1425, Nov. 2009.

[7] P. K. Mallick, *Fiber-reinforced composites : materials, manufacturing, and design*, 3rd ed. Boca Raton, FL: CRC Press.

[8] D. Stavrov and H. E. N. Bersee, "Resistance welding of thermoplastic composites-an overview," *Composites Part A: Applied Science and Manufacturing*, vol. 36, no. 1, pp. 39–54, Jan. 2005.

[9] National Aerospace Standard, Ed., "NASM1312: Fastener Test Methods." 1997.

[10] Department of Defense of the United States of America, *Military Handbook: Metallic Materials and Elements for Aerospace Vehicle Structures*. 1998.

[11] F. Lapointe, A. Oswalt, A. Nakai, and L. Laberge Lebel, "Manufacturing of Carbon/Polyamide Beam by Vacuum Assisted Pultrusion," presented at the ECCM17 - 17th European Conference on Composite Materials, Munich, Germany, 2016.

[12] W. S. Rasband, *ImageJ*. Bethesda, Maryland, USA: U. S. National Institutes of Health, 2016.